

Compositional and Isotopic Characteristics for The Longmaxi Shale Gas in The Northern Guizhou Area, South China

Wenting Jiang

Guizhou University

Peng Xia (✉ pxia@gzu.edu.cn)

Guizhou University

Qingguang Li

Guizhou University

Yong Fu

Guizhou University

Yuliang Mou

Guizhou University

Research

Keywords: Shale gas, Carbon isotope, Molecular composition, Longmaxi formation, Northern Guizhou area

Posted Date: November 10th, 2020

DOI: <https://doi.org/10.21203/rs.3.rs-102585/v1>

License: © ⓘ This work is licensed under a Creative Commons Attribution 4.0 International License. [Read Full License](#)

Abstract

The organic-rich marine shale of the Lower Silurian Longmaxi formation in the northern Guizhou area (NGA), China, is characterized by its high thermal maturity (R_o values range in 2.18%~3.12%), high TOC values (0.92%~4.87%), high gas contents (0.47~2.69 m³/t) and type II₁ organic matter, and has recently been a precursor for shale gas exploration and development. Compositional and isotopic parameters of 7 gas samples from Longmaxi shale from DY-1 well were analyzed in this study. Dry coefficient of the gases is up to 30~200 making the northern Guizhou Longmaxi shale gas among the driest gaseous hydrocarbons in the world. The $\delta^{13}\text{C}_{\text{CH}_4}$ values range from -38.6‰ to -18.6‰ and the $\delta^{13}\text{C}_{\text{C}_2\text{H}_6}$ values vary in -36.2‰~-30.8‰. These results indicate that the Longmaxi shale gas is of thermogenic origin and oil derived. This Longmaxi shale gas has high proportion of non-hydrocarbon gases especially including nitrogen in response to complicate tectonic movements and strong hydrodynamic flushing. Tectonic movement and hydrodynamic flushing not only destroy hydrocarbon gases reservoirs but also change the isotope distribution of gaseous hydrocarbons. Isotopic reversal is frequent in closed system, and under relatively bad preserving condition, the isotope distribution will back to normal even at overmature evolution stage.

1. Introduction

Chemical and isotopic compositions are two key parameters for characterizing natural gases (Dai et al., 2012). Theoretical and empirical evidences demonstrate that cogenetic gases commonly obey the relationship of methane $\delta^{13}\text{C}$ ($\delta^{13}\text{C}_1$) < ethane $\delta^{13}\text{C}$ ($\delta^{13}\text{C}_2$) < propane $\delta^{13}\text{C}$ ($\delta^{13}\text{C}_3$) (McCollom et al., 2010). However, in the last few years, abnormal geochemical characteristics including the “rollover” of ethane and propane $\delta^{13}\text{C}$ values, carbon isotopic reversals and extremely high proportion of non-hydrocarbon gases have been found in various unconventional gas reservoirs especially including productive gas shales (Zumberge et al., 2012; Dai et al., 2014; Liu et al., 2016). The molecular composition of shale gas, which is determined by its organic matter type, thermal maturity and preservation condition, is mainly including methane (CH₄), ethane (C₂H₆), propane (C₃H₈), nitrogen (N₂) and carbon dioxide (CO₂), and the volumetric contents of methane (CH₄), ethane (C₂H₆), propane (C₃H₈), nitrogen (N₂) and carbon dioxide (CO₂) in shale gases frequently range in 11.55% ~ 99.59%, 0.01% ~ 23.96%, 0.01% ~ 38.35%, 0.01% ~ 15.84% and 0.01% ~ 14.82%, respectively, according to the existing reports (Martini et al., 2008; Zhao et al., 2016). During the immature stage of thermal maturity ($R_o < 0.5\%$), kerogen is degrading into biogenic gas (mainly including methane), and it is decomposing into thermogenic gases (e.g. methane, ethane and propane) during mature stage ($1.0\% < R_o < 2.0\%$) (Fig. 1). Oil-primary cracking gradually generates heavy hydrocarbon gases (e.g. ethane and propane) after mature stage, and these heavy hydrocarbon gases will be cracked again (oil-secondary cracking) in overmature stage ($R_o > 2.0\%$) and transfer into methane (Xue et al., 2015). The $\delta^{13}\text{C}$ values of these gaseous hydrocarbons follow general orders of (1) thermogenic methane < thermogenic ethane < thermogenic propane (normal carbon isotopic distribution) (2) primary oil-cracking ethane and propane < thermogenic methane < secondary oil-cracking ethane and propane (Dai et al., 2012; Xia et al., 2013). Mixing of these different kinds of gases causes the isotopic reversals (Dai et al., 2014).

Isotopic reversals and molecular compositions of shale gas are helpful for reflecting its origin and preserve condition. Dai (1993) and Sherwood et al. (2008) discovered that $\delta^{13}\text{C}$ methane maintain increase but $\delta^{13}\text{C}$ ethane and propane will decrease due to oil-primary cracking with increasing thermal maturity, which is one reason of isotopic reversals. Hao and Zou (2013) reported that isotopic reversals usually occur in closed-system shales. Martini et al. (2003) and Zhao et al. (2016) concluded that the tectonic movement and hydrodynamic flushing represent poor preserve condition and make gaseous hydrocarbons desorbed and increase the contents of non-hydrocarbon gases.

The northern Guizhou area (NGA) (Fig. 2), which was selected as a precursor of shale gas by the state of Guizhou province and the Ministry of Land and Resources (MLR), is located to the south of the Sichuan basin. The marine black shales are widely distributed in the Lower Silurian Longmaxi formation in the NGA. The Longmaxi organic-rich shale has experienced complicated tectonic movements, which bring difficult to analyze its hydrocarbon generation history and gas preservation condition (Dai et al., 2015). In recent years, significant attention has been paid to the Longmaxi organic-rich shale in the NGA, however, these researches mainly concerned its sedimentary, mineralogical, geochemical and geophysical properties. The isotopic and compositional characteristics of gas itself were discussed rarely. The objective of this study is to determine the origin of hydrocarbon gases and discuss the implications of carbon isotopic reversals, based on the molecular and stable carbon isotope compositions of gaseous hydrocarbons.

2. Samples And Experiments

A total of 7 Longmaxi shale core samples (their fundamental information and main organic geochemical parameters can be seen in Table 1) were collected from shale gas well DY-1 in the NGA, and these fresh samples were placed immediately inside a hermetically sealed canister immersed in a water bath at the reservoir temperature. The volumes of gas released inside the canister were measured using a graduated cylinder at atmospheric pressure, and the loss gas volumes were evaluated by the method in Tang et al. (2011). The gas samples were collected from the released gas, which has been considered as mixture of adsorbed and free gases (Liu et al., 2016).

Table 1
Primary information and organic geochemical parameters of shale samples.

| Sample | Depth (m) | GC (m ³ /t) | TOC (%) | R _o (%) | S ₁ (mg/g) | S ₂ (mg/g) | T _{max} (°C) | PI | Sa (%) | In (%) | Vi (%) | KT |
|--------|--------------|---------------------------|------------|-----------------------|--------------------------|--------------------------|--------------------------|------|-----------|-----------|-----------|-----------------|
| S1 | 533.0 | 1.84 | 0.97 | 2.57 | 0.01 | 0.04 | 354 | 0.2 | 12 | 85 | 3 | II ₁ |
| S2 | 557.0 | 0.47 | 0.92 | 3.06 | 0.01 | 0.03 | 355 | 0.25 | 10 | 88 | 2 | II ₁ |
| S3 | 560.0 | 0.71 | 3.22 | 2.60 | 0.03 | 0.09 | 368 | 0.25 | 16 | 83 | 1 | II ₁ |
| S4 | 573.0 | 2.17 | 3.61 | 2.73 | 0.04 | 0.09 | 377 | 0.3 | 10 | 87 | 3 | II ₁ |
| S5 | 589.5 | 2.41 | 4.87 | 2.51 | 0.04 | 0.06 | 364 | 0.4 | 9 | 89 | 2 | II ₁ |
| S6 | 593.0 | 2.69 | 4.60 | 3.12 | 0.08 | 0.18 | 368 | 0.31 | 6 | 89 | 5 | II ₁ |
| S7 | 597.0 | 2.03 | 4.63 | 2.18 | 0.06 | 0.17 | 462 | 0.26 | 10 | 87 | 3 | II ₁ |

Note: GC is gas content; Sa is sapropelite; In is inertinite; Vi is vitrinite and KT is kerogen type.

The molecular compositions of gas samples diluted in hydrogen were determined using an Agilent 6890N gas chromatograph (GC) equipped with a flame ionization and a thermal conductivity detector in Research Institute of Petroleum Exploration & Exploitation. The GC oven temperature was initially set at 70 °C for 10 min and then increased to 130 °C at 15 °C/min. A single hydrocarbon gas component was separated by capillary column of 50 m length × 0.53 mm diameter. Stable carbon isotopic analyses for separated C₁-C₃ hydrocarbon gases were performed in Research Institute of Petroleum Exploration & Exploitation on the Thermo Delta V Advantage isotope mass spectrometer (IMS). The stable carbon isotopic data were presented in δ -notation ($\delta^{13}\text{C}$, ‰) relative to VPDB standard, and each sample was measured in triplicate with a precision of less than $\pm 0.5\text{‰}$. The molecular compositions and stable carbon isotopic values of gas samples are documented in Table 2.

Table 2
Molecular and isotopic compositions of shale gas samples.

| Sample | Molecular compositions (%) | | | | | | $\delta^{13}\text{C}$ (% VPBD) | | |
|--------|----------------------------|-------------------------------|-------------------------------|-----------------|----------------|----------------|--------------------------------|-------------------------------|-------------------------------|
| | CH ₄ | C ₂ H ₆ | C ₃ H ₈ | CO ₂ | O ₂ | N ₂ | CH ₄ | C ₂ H ₆ | C ₃ H ₈ |
| S1 | 18.85 | 1.27 | 0.22 | 0.55 | 14.54 | 64.57 | nm | nm | nm |
| S2 | 78.36 | 0.43 | nd | 0.87 | 4.37 | 15.97 | -31 | -34 | nm |
| S3 | 54.17 | 2.8 | 1.06 | 2.05 | 7.9 | 32.02 | -18.6 | -30.8 | -35.9 |
| S4 | 38.22 | 1.44 | nd | 0.69 | 12.4 | 47.25 | nm | nm | nm |
| S5 | 88.91 | 0.46 | nd | 0.68 | 2.39 | 7.56 | -36.7 | -35.3 | nm |
| S6 | 46.83 | 1.12 | nd | 1.29 | 10.63 | 40.13 | nm | nm | nm |
| S7 | 47.22 | 1.55 | nd | 1.04 | 10.18 | 40.01 | -38.6 | -36.2 | nm |

Note: nd is not detected; nm is not measured.

3. Results

As shown in Table 1, the organic matters of the shale samples used in this study are in the overmature stage with R_o of 2.18%~3.12%, indicating that the organic matters evolved into a dry gas window. Visual assessment of the organic matter reveals that the kerogen type index (TI) ranges from 47 to 57, which confirms that humic-sapropelic (II₁) as the kerogen type. TOC contents of these shale samples vary from 0.92–4.87%, and have a significantly positive correlation with the burial depth. The gas contents range from 0.47 m³/t to 2.69 m³/t with an average of 1.76 m³/t.

3.1. Molecular composition of shale gas

As can be seen in Table 2, the released gas from the 7 shale samples is mainly composed of methane and nitrogen. Methane accounts for 18.85–88.91% (averaging 53.22%) and nitrogen contents vary from 7.56–64.57% (averaging 35.36%) in the molecular compositions. The gas samples have very low C₂₊ components (heavy hydrocarbon gases) with small amount of ethane ranging from 0.43–2.80% and no or only trace propane (0 ~ 1.06%). The contents of carbon dioxide and oxygen are 0.55%~2.05% (averaging 1.02%) and 2.39%~14.54% (averaging 8.92%), respectively, while no hydrogen sulfide was detected. Compared with the adjacent Sichuan basin (Dai et al., 2014), the Longmaxi shale gas in the NGA is characterized by its abnormally high contents of nitrogen and oxygen, even though they have no notable difference in TOC, R_o value and heavy hydrocarbon gases content.

3.2. Stable carbon isotopic composition of shale gas

As shown in Table 2, the $\delta^{13}\text{C}_1$ values of the gas samples in this study vary from -36.2‰ to -18.6‰ with an average of -31.2‰, which is much wider and abnormal than those in the adjacent Sichuan basin (Feng et al., 2016). The carbon isotopic composition of ethane in primary natural gas has been considered as having an

outstanding parent material inheritance, and the $\delta^{13}\text{C}_2$ values of oil-type and coal-derived gases are $< -29\text{‰}$ and $> -28\text{‰}$, respectively (Gang et al., 1997). The $\delta^{13}\text{C}_2$ values of our gas samples range from -36.2‰ to -30.8‰ (averaging -34.1‰), which reflect an oil-derived characteristic. Dai et al. (2014) reported that the phenomenon of $\delta^{13}\text{C}_1 > \delta^{13}\text{C}_2$ (isotopic reversal) is common in the Sichuan basin, which has a close relationship with the high maturity of Longmaxi shale. Even though Longmaxi shales in the Sichuan basin and NGA have a similar R_o distribution, the relationship of $\delta^{13}\text{C}_1$ and $\delta^{13}\text{C}_2$ is much complicated in the NGA than that in the Sichuan basin. As shown in Fig. 3, two of our gas samples (S5 and S7) have normal carbon isotope distribution ($\delta^{13}\text{C}_1 < \delta^{13}\text{C}_2$). Compared to S5 and S7, the others two samples (S2 and S3) have notably heavier carbon isotope and reversed carbon isotope distribution ($\delta^{13}\text{C}_1 > \delta^{13}\text{C}_2 > \delta^{13}\text{C}_3$).

4. Discussions

4.1. Origin of alkane gases

Three genetic types of hydrocarbon gas (biogenic, thermogenic and mixed gases) can be identified using its molecular composition and carbon isotopes (Dai, 1993). Low $\delta^{13}\text{C}_1$ value (usually, $< -55\text{‰}$) and high methane content (usually, > 1 mol/L) are two recognizing characteristics of biogenic gas (Martini et al., 2003). Compared with biogenic gas, thermogenic gas has a much higher $\delta^{13}\text{C}_1$ value and a notable relationship of $\delta^{13}\text{C}_1$ value and thermal maturity (Dai, 2011). Figure 4 shows a cross plot of gas molecular composition and carbon isotope of gaseous alkanes from the northern Guizhou Longmaxi shale gases, and reflects that the shale gas samples in the NGA, as well as the adjacent Sichuan basin (Feng et al., 2016) and Barnett and Fayetteville shale gases (Zumberge et al., 2012), are oil-derived thermogenic gas.

Wu et al. (2011) reported that coal-derived gas in the Sichuan basin has a negative correlation of $\delta^{13}\text{C}_1$ value and thermal maturity. Even though all Barnett, Fayetteville and Longmaxi shale gases in the Sichuan basin and NGA are oil-derived thermogenic gas, the Longmaxi shale gases have both higher thermal maturity and $\delta^{13}\text{C}_1$ value and belong to cracking gas, and a large part of Barnett and Fayetteville shale gases are associated gas. As can be seen in Fig. 1, oil-cracking gas has higher thermal maturity than associated gas, and is composed of primary (condensate gas) and secondary (dry gas) oil-cracking gases. In this study, the organic matters are in the overmature stage with R_o of 2.18%~3.12% (Table 1), indicating that the organic matters evolved into a dry gas window. As a result, the gaseous hydrocarbon of northern Guizhou Longmaxi shale contains very low heavy hydrocarbon gases and large proportion of methane.

4.2. Isotopic rollovers and reversals

With the recent exploration and development successes in shale gas, it has been demonstrated that isotopic rollover and reversal are more commonplace in shale gas than in conventional reservoir (Zhao et al., 2016). The “rollover” means that the isotopic compositions change with increasing thermal maturity, and the “reversal” refers to that carbon isotopic sequence do not follow the normal carbon isotopic sequence ($\delta^{13}\text{C}_1 < \delta^{13}\text{C}_2 < \delta^{13}\text{C}_3$) (Strapoc et al., 2010). A complete and a partial carbon isotopic reversals of n-alkane gases are

probably due to (1) mixing of different origins of gases, (2) mixing of different types of gases, (3) the influence of oil and associated gas cracking (Martini et al., 2008; Dai et al., 2014).

Figure 5 shows a cross plot of $\delta^{13}\text{C}_1$ and $\delta^{13}\text{C}_2$ values, which reflects that all gases from the Antrim shale (R_o value is 0.4%~0.6%), New Albany shale (R_o value is 0.4%~1.0%) and Jurassic shale in Jafurah basin (R_o is 1.00%~1.55%), and most gases from the Barnett shale (R_o value is 0.5%~2.0%) have normal carbon isotope distribution ($\delta^{13}\text{C}_1 < \delta^{13}\text{C}_2$), whereas all gases from the Fayetteville shale (R_o value is 1.25%~4.00%), Lower Cambrian shale (R_o value is 2.2%~3.5%) and Wufeng-Longmaxi shale (R_o value is 2.1%~3.2%) in the Sichuan basin display isotopic reversals ($\delta^{13}\text{C}_1 > \delta^{13}\text{C}_2$). That is to say the thermal maturity has dominating effect on carbon isotopic reversal, and higher thermal evolution gas has more possibility to exhibit reversal. Owing to the reservoir openness and the effects from migration fractionation, the conventional natural gases in the Sichuan basin follow the normal distribution even though its high thermal maturity (R_o value is 2.2%~3.5%). Closed shale system is another prerequisite for isotopic reversal (Golding et al., 2013). As shown in Fig. 6, with the increasing dry coefficient ($C_1/(C_2 + C_3)$), which can reflect thermal maturity, both ethane and propane $\delta^{13}\text{C}$ values have two carbon isotopic rollovers (Burruss and Laughrey, 2010). All methane, ethane and propane $\delta^{13}\text{C}$ values increase with increasing $C_1/(C_2 + C_3)$ when $C_1/(C_2 + C_3)$ lower than about 20, and they have normal isotopic distribution ($\delta^{13}\text{C}_1 < \delta^{13}\text{C}_2 < \delta^{13}\text{C}_3$). The ethane and propane $\delta^{13}\text{C}$ values begin to decrease (become isotopically lighter, the first rollover) at $C_1/(C_2 + C_3)$ around 20 due to the effect of oil and condensate cracking (Jarvie et al., 2007), and methane $\delta^{13}\text{C}$ value maintains increase since it mainly generated by biological degradation (Martini et al., 1998). The second rollover occurred due to the decomposition of ethane and propane (Hill et al., 2003). Ethane and propane begin to decompose into methane at high thermal maturity (maybe corresponding R_o value is higher than 2.0%), and ^{12}C ethane and ^{12}C propane are much easier decomposed than ^{13}C ethane and ^{13}C propane due to their weaker polarity (Zumberge et al., 2012).

As shown in Fig. 5, only a half of our samples (S2 and S3) are reversed ($\delta^{13}\text{C}_1 > \delta^{13}\text{C}_2$), and the others samples (S5 and S7) follow normal isotopic distribution ($\delta^{13}\text{C}_1 < \delta^{13}\text{C}_2$) even though they are overmatured with R_o values (Table 1) are approximated to those of the Wufeng-Longmaxi shale in the Sichuan basin. The main reasons of those odd normal isotopic distributions are the inferior preserving condition of reservoir. Large faults zones and the flash of spring water in them have damaged or even destroyed the shale gas reservoir, and as a result, the contents of non-hydrocarbon gases are prodigiously high and the evolution trend of carbon isotopes of alkane gases are disorganized.

4.3. Geological implications

Shale gas usually consists of methane, small amounts of heavy hydrocarbon gases ($\text{C}_2\text{-C}_6$) and non-hydrocarbon gases (CO_2, N_2). The proportion of heavy hydrocarbon gases ($\text{C}_2\text{-C}_6$) tend to decrease with increasing thermal maturity (Zhang et al., 2014), and the proportion of non-hydrocarbon gases (CO_2, N_2) are mainly affected by tectonic movement and hydrodynamic condition (Dai et al., 2008). As shown in Fig. 7, Barnett shale gas, Fayetteville shale gas and Longmaxi-Wufeng shale gas in the Sichuan basin are rich in methane and have been successfully developed, in which the methane percentage contents are no less than

80% (Zumberge et al., 2012; Dai et al., 2016). Martini et al. (2008) reported that New Albany shale gas has large proportion of ethane and propane (the content of ethane + propane can exceed 45%) due to its low thermal maturity (R_o value is 0.4%~1.0%). However, Martini et al. (1998, 2003) also found that Antrim shale gas has relative lower proportion of heavy hydrocarbon gases but rich in N_2 and CO_2 even though its thermal maturity (R_o value is 0.4%~0.6%) is little lower than that of New Albany shale gas, and they believed that this phenomenon has been caused by the effect of Pleistocene glaciation. Our samples also have very little heavy hydrocarbon gases and rich in N_2 and CO_2 , however, the differences between our samples and Antrim shale are (1) thermal maturity is much higher than Antrim shale, (2) no glaciation but large faults zones and springs are widespread (Fig. 2). Heavy hydrocarbon gases are gradually decomposed into methane in overmatured stage, and the faults zones and springs generated by tectonic movement damage gas reservoir. As a result, northern Guizhou Longmaxi shale gas is rich in non-hydrocarbon gases, and is lack of heavy hydrocarbon gases. Owing to their same tectonic evolution history and geological background, the Lower Cambrian shale, which is another important organic-rich black shale in the NGA, has the same molecular composition with the Longmaxi shale.

As shown in Fig. 6, carbon isotopic distribution changes with increasing thermal maturity. At lower thermal maturity, kerogen cracking in a closed system resulted in increasing ethane ^{13}C and propane (Zhao et al., 2016). At relatively high thermal maturity, simultaneous cracking of kerogen, retained oil and condensate resulted in rollover of ethane $\delta^{13}C$ and propane $\delta^{13}C$, and the resultant conversion of isotopic distribution patterns from normal though partial reversal to complete reversal. Carbon isotopic distribution can be used to distinguish gas origins combined with molecular composition. The isotopic reversal demonstrates a closed shale system, which has a better preserving condition than opened system (Xia et al., 2018). The larger the reversal degree is, the higher the gas content is. Moreover, the carbon isotopic distribution is also useful to evaluate reservoir preserve condition. Isotopic reversal is frequent in closed system, and under relatively bad preserving condition, the isotopic distribution will back to normal even at overmature evolution stage.

5. Conclusions

The northern Guizhou Longmaxi shale gas has abnormal high proportion of non-hydrocarbon gases especially including nitrogen as the result of complicate tectonic movements and strong hydrodynamic flushing, and is of thermogenic origin and oil-derived. The northern Guizhou Longmaxi shale gas evolved into dry gas window with R_o value is ranging in 2.18%~3.12%, which is close to the thermal maturity of Longmaxi shale in the adjacent Sichuan basin (2.1%~3.2%). Even though they have a similar thermal maturity distribution, the northern Guizhou Longmaxi shale gas has abnormal high proportion of non-hydrocarbon gases (e.g. nitrogen) compared with the Sichuan basin Longmaxi shale gas due to the effects from complicate tectonic movements and strong hydrodynamic flushing. Tectonic movement and hydrodynamic flushing not only destroy hydrocarbon gases reservoirs but also change the isotope distribution of gaseous hydrocarbons. Isotopic reversal is frequent in closed system, and under relatively bad preserving condition, the isotope distribution will back to normal even at overmature evolution stage.

Declarations

The authors declare that they have no known competing financial interest that could have appeared to influence the work reported in this paper.

Acknowledgements

This work was financially supported by the program of National Natural Science Foundation of China (Nos. 42002166, 42063009, 41867050).

References

1. Burruss, R. C., and Laughrey, C. D. 2010. Carbon and hydrogen isotopic reversals in deep basin gas: evidence for limits to the stability of hydrocarbons. *Organic Geochemistry*, 42: 1285-1296.
2. Dai, C. G., Hu, M. Y., Chen, J. S., Wang, M., and Wang, X. H. 2015. The important geologic events of Guizhou province and its geologic significance. *Guizhou Geology (in Chinese)*, 32(1): 1-14.
3. Dai, J. X. 1993. The characteristics of carbon and hydrogen isotope of natural gas. *Natural Gas Geoscience (in Chinese)*, (Z1): 1-40.
4. Dai, J. X. 2011. Significance of the study on carbon isotopes of alkane gases. *Natural Gas Industry (in Chinese)*, 31(12): 1-6.
5. Dai, J. X., Ni, Y. Y., and Zou, C.N. 2012. Stable carbon and hydrogen isotopes of natural gases sourced from the Xujiahe Formation in the Sichuan Basin, China. *Organic Geochemistry*, 43: 103-111.
6. Dai, J. X., Zou, C. N., Dong, D. Z., Ni, Y. Y., Wu, W., Gong, D. Y., Wang, Y. M., Huang, S. P., Huang, J. L., Fang, C. C., and Liu, D. 2016. Geochemical characteristics of marine and terrestrial shale gas in China. *Marine and Petroleum Geology*, 76: 444-463.
7. Dai, J. X., Zou, C. N., Liao, S. M., Dong, D. Z., Ni, Y. Y., Huang, J. L., Wu, W., Gong, D. Y., Huang, S. P., and Hu, G. Y. 2014. Geochemistry of the extremely high thermal maturity Longmaxi shale gas, southern Sichuan basin. *Organic Geochemistry*, 74: 3-12.
8. Feng, Z. Q., Liu, D., Huang, S. P., Wu, W., Dong, D. Z., Peng, W. L., and Han, W. X. 2016. Carbon isotopic composition of shale gas in the Silurian Longmaxi formation of the Changning area, Sichuan basin. *Petroleum Exploration and Development (in Chinese)*, 43(5): 705-713.
9. Gang, W. Z., Gao, G., Hao, S. S., Huang, Z. L., and Zhu, L. 1997. Carbon isotope of ethane applied in the nalysis of genetic types of natural gas. *Experimental Petroleum Geology (in Chinese)*, 19(2): 164-167.
10. Golding, S. D., Boreham, C. J., and Esterle, J. S. 2013. Stable isotope geochemistry of coal bed and shale gas and related production waters: A review. *International Journal of Coal Geology*, 120: 24-40.
11. Hao, F., and Zou, H. Y. 2013. Cause of shale gas geochemical anomalies and mechanisms for gas enrichment and depletion in high-maturity shales. *Marine and Petroleum Geology*, 44: 1-12.
12. Hill, R. J., Tang, Y. C., and Kaplan, I. R. 2003. Insights into oil cracking based on laboratory experiments. *Organic Geochemistry*, 34: 1651-1672.
13. Jarvie, D. M., Hill, R. J., Ruble, T. E., and Pollastro, R. M. 2007. Unconventional shale-gas systems: The Mississippian Barnett Shale of north-central Texas as one model for thermogenic shale-gas assessment. *AAPG Bulletin*, 91(4): 475-499.

14. Liu, Y., Zhang, J. C., Ren, J., Liu, Z. Y., Huang, H., and Tang, X. 2016. Stable isotope geochemistry of the nitrogen-rich gas from lower Cambrian shale in the Yangtze Gorges area, South China. *Marine and Petroleum Geology*, 77: 693-702.
15. Martini, A. M., Walter, L. M., Budai, J. M., Ku, T. C. W., Kaiser, C. J., and Schoell, M. 1998. Genetic and temporal relations between formation waters and biogenic methane: Upper Devonian Antrim Shale, Michigan Basin, USA. *Geochimica et Cosmochimica Acta*, 62(10): 1699-1720.
16. Martini, A. M., Walter, L. M., and McIntosh, J. C. 2008. Identification of microbial and thermogenic gas components from Upper Devonian black shale cores, Illinois and Michigan basins. *AAPG Bulletin*, 92(3): 327-339.
17. Martini, A. M., Walter, L. M., Ku, T. C. M., Budai, J. M., McIntosh, J. C., and Schoell, M. 2003. Microbial production and modification of gases in sedimentary basins: A geochemical case study from a Devonian shale gas play, Michigan basin. *AAPG Bulletin*, 87(8): 1355-1375.
18. McCollom, T. M., Lollar, B. S., Lacrampe-Couloume, G., and Seewald, J. S. 2010. The influence of carbon source on abiotic organic synthesis and carbon isotope fractionation under hydrothermal conditions. *Geochimica et Cosmochimica Acta*, 74: 2717-2740.
19. Strapoc, D., Mastalerz, M., Schimmelmann, A., Drobniak, A., and Hasenmueller, N. R. 2010. Geochemical constraints on the origin and volume of gas in the New Albany Shale (Devonian–Mississippian), eastern Illinois Basin. *AAPG Bulletin*, 94(11): 1713-1740.
20. Tang, Y., Zhang, J. C., Liu, Z. J., and Li, L. Z. 2011. Use and improvement of the desorption method in shale gas content tests. *Natural Gas Industry (in Chinese)*, 31(10): 108-112.
21. Wu, W., Xie, J., Shi, X. W., Zhao, S. X., Ji, C. H., Hu, Y., and Guo, Y. B. 2017. Accumulation condition and exploration potential for Wufeng-Longmaxi shale in Wuxi area, northeastern Sichuan basin. *Natural Gas Geoscience (in Chinese)*, 28(5): 734-743.
22. Wu, X. Q., Huang, S. P., Liao, F. R., and Li, Z. S. 2011. Carbon isotopic compositions of coal-derived gas in the Xujiahe formation and Jurassic in the Sichuan basin. *Petroleum Exploration and Development (in Chinese)*, 38(4): 418-427.
23. Xia, P., Wang, G. L., Zeng, F. G., Mou, Y. L., Zhang, H. T., and Liu, J. G. 2018. The characteristics and mechanism of high-over matured nitrogen-rich shale gas of Niutitang formation, northern Guizhou area. *Natural Gas Geoscience (in Chinese)*, 29(9): 1345-1355.
24. Xia, X. Y., Chen, J., Braun, R., and Tang, Y. C. 2013. Isotopic reversals with respect to maturity trends due to mixing of primary and secondary products in source rocks. *Chemical Geology*, 339: 205-212.
25. Xue, L. H., Yang, W., Zhong, J. A., Xu, Y., and Chen, G. J. 2015. Porous evolution of the organic-rich shale from simulated experiment with geological constraints, samples from Yanchang formation in Ordos basin. *Acta Geologica Sinica*, 89(5): 970-978.
26. Zhang, T. W., Yang, R. S., Milliken, K. L., Ruppel, S. C., Pottorf, R. J., and Sun, X. 2014. Chemical and isotopic composition of gases released by crush methods from organic rich mudrocks. *Organic Geochemistry*, 73: 16-28.
27. Zhao, J. Z., Pu, B. L., Er, C. Shale gas and shale gas geochemistry. East China University of Science and Technology Press, Shanghai, China, 2016.

28. Zumberge, J., Ferworn, K., and Brown, S. 2012. Isotopic reversal ('rollover') in shale gases produced from the Mississippian Barnett and Fayetteville formations. *Marine and Petroleum Geology*, 31: 43-52.

Figures

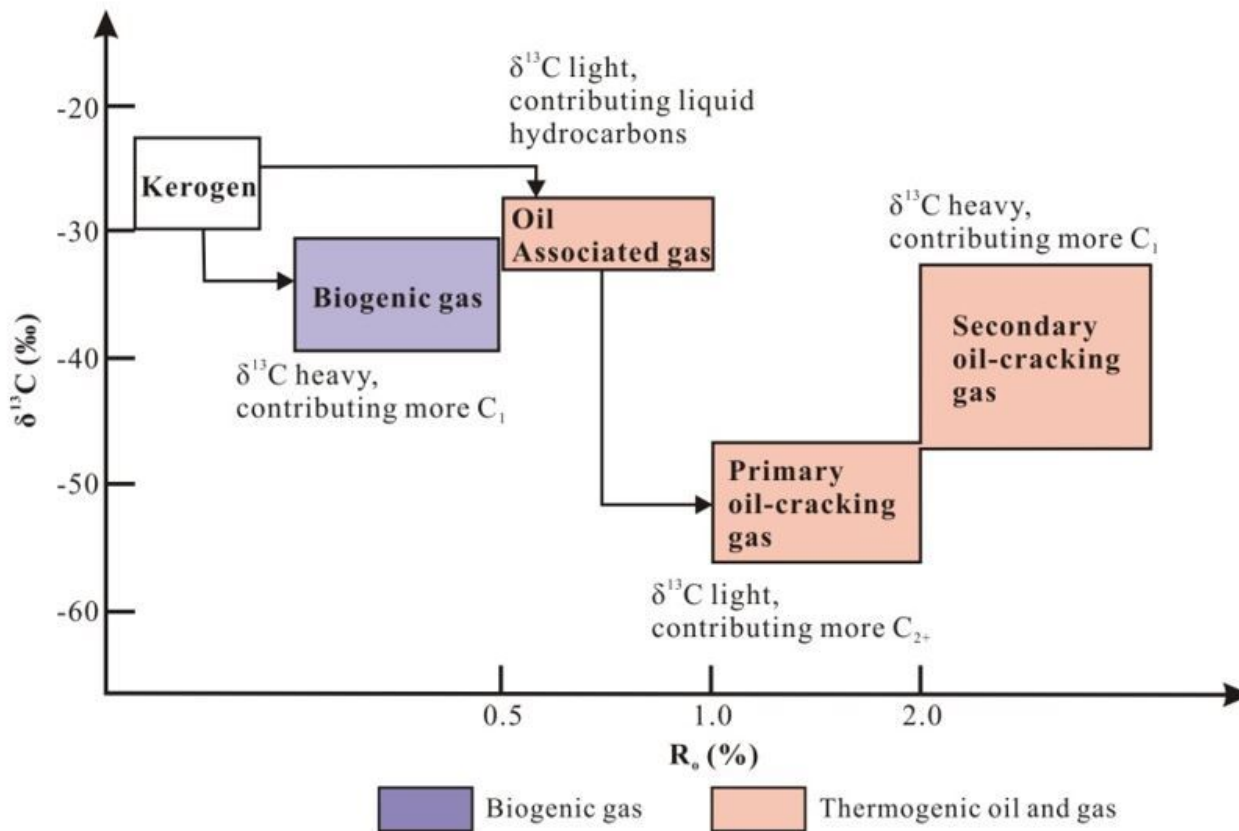


Figure 1

Scheme showing hydrocarbon products during different thermal evolution stages.

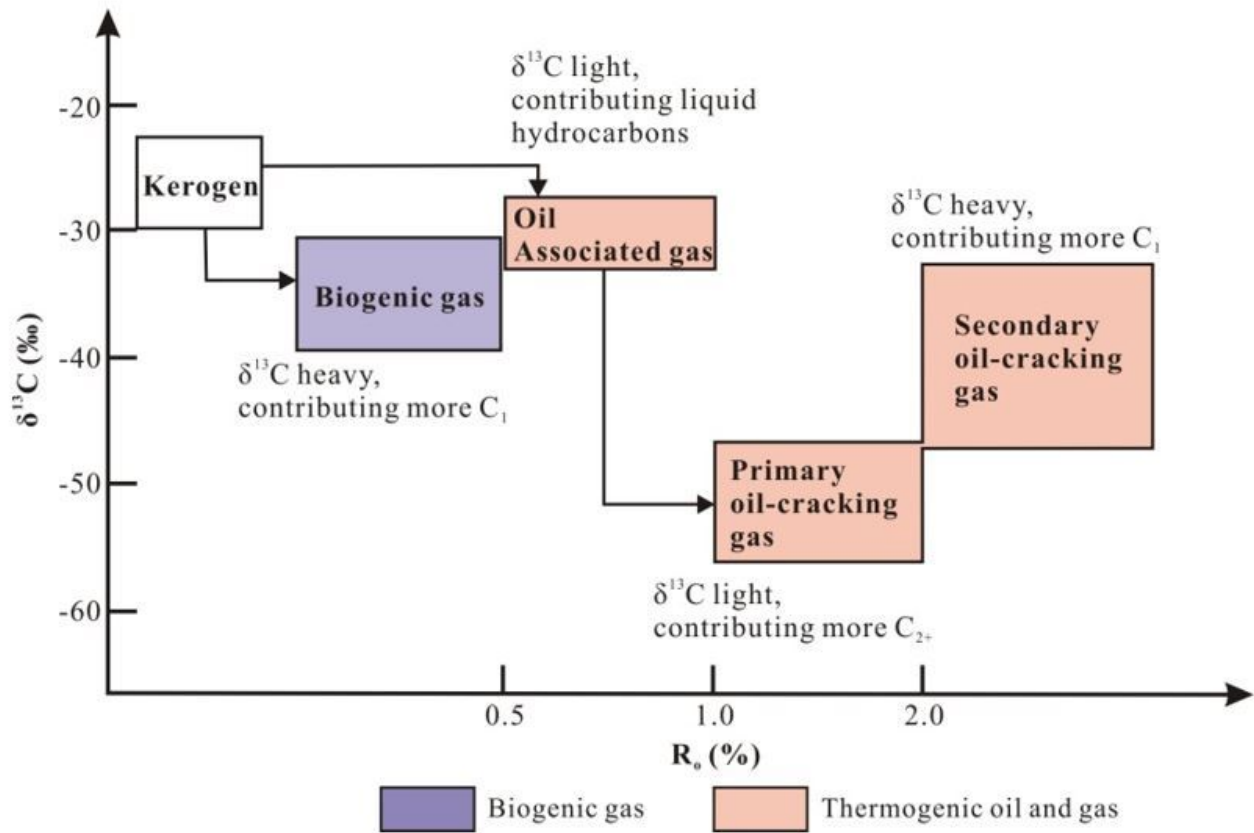


Figure 1

Scheme showing hydrocarbon products during different thermal evolution stages.

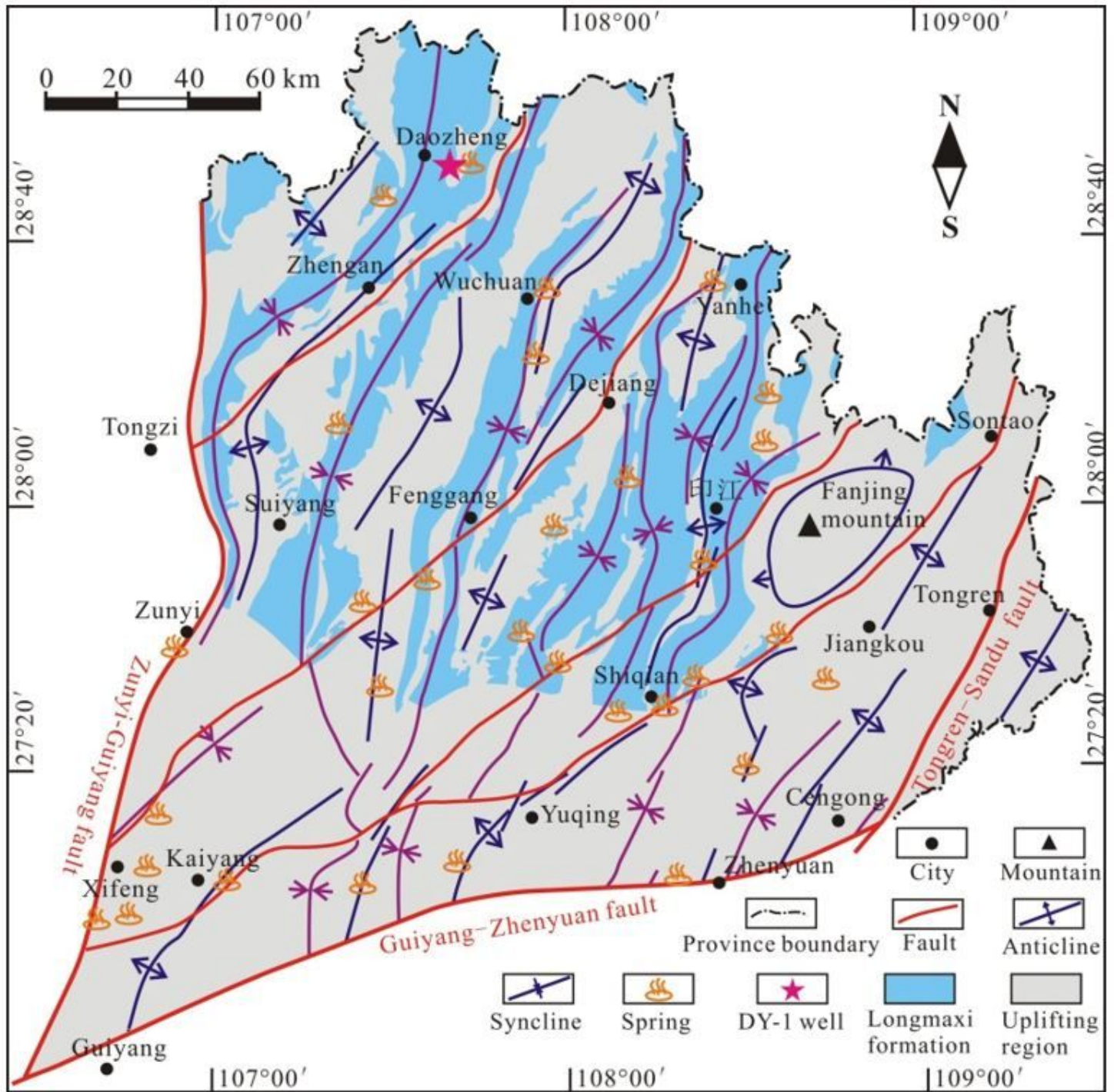


Figure 2

Structural sketch and the distribution of the Longmaxi formation in the NGA (revised from Resources Prospecting Reports, Chengdu Institute of Geology and Mineral Resources, 2014, <http://www.chengdu.cgs.gov.cn/>). Note: The designations employed and the presentation of the material on this map do not imply the expression of any opinion whatsoever on the part of Research Square concerning the legal status of any country, territory, city or area or of its authorities, or concerning the delimitation of its frontiers or boundaries. This map has been provided by the authors.

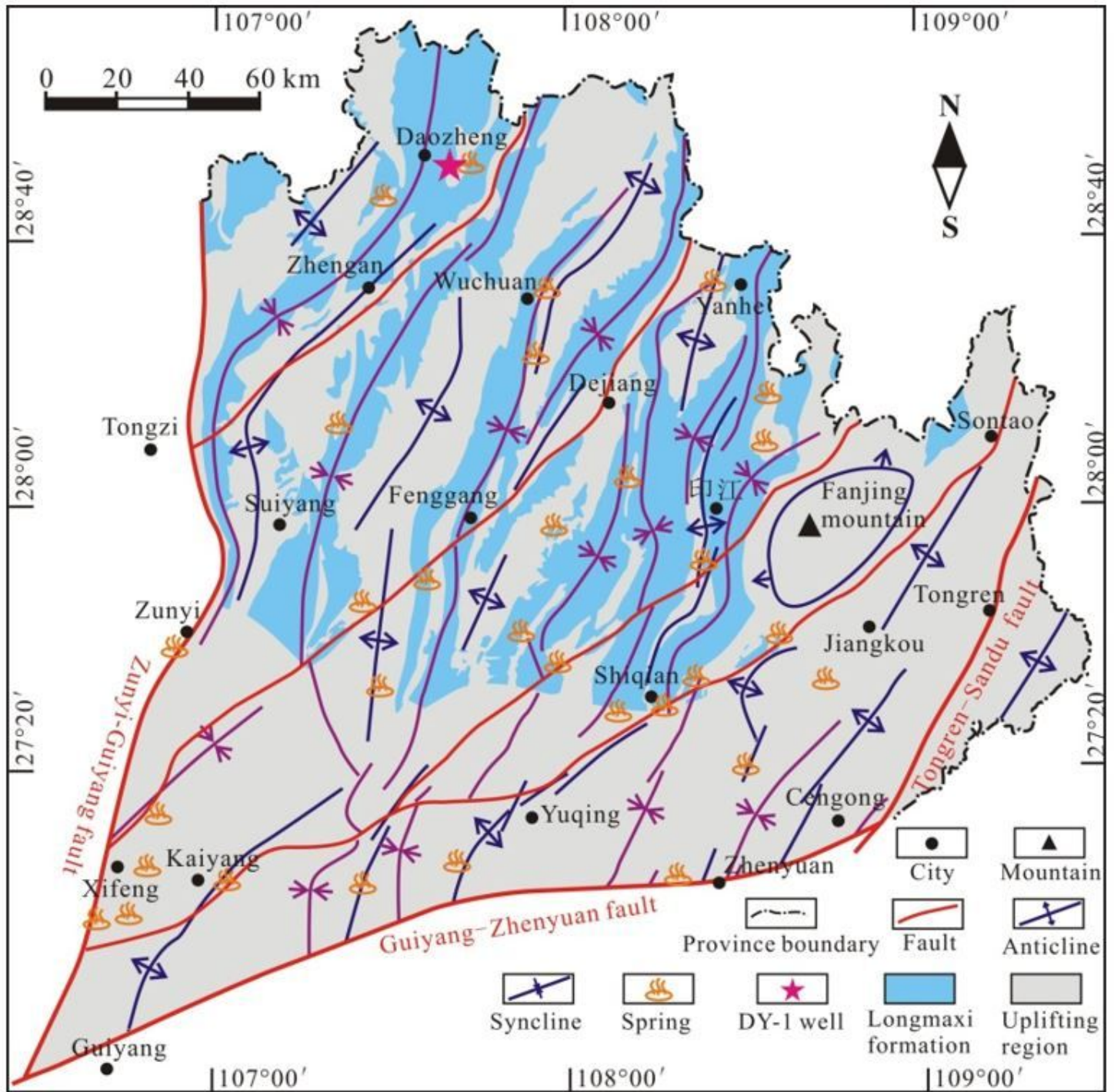


Figure 2

Structural sketch and the distribution of the Longmaxi formation in the NGA (revised from Resources Prospecting Reports, Chengdu Institute of Geology and Mineral Resources, 2014, <http://www.chengdu.cgs.gov.cn/>). Note: The designations employed and the presentation of the material on this map do not imply the expression of any opinion whatsoever on the part of Research Square concerning the legal status of any country, territory, city or area or of its authorities, or concerning the delimitation of its frontiers or boundaries. This map has been provided by the authors.

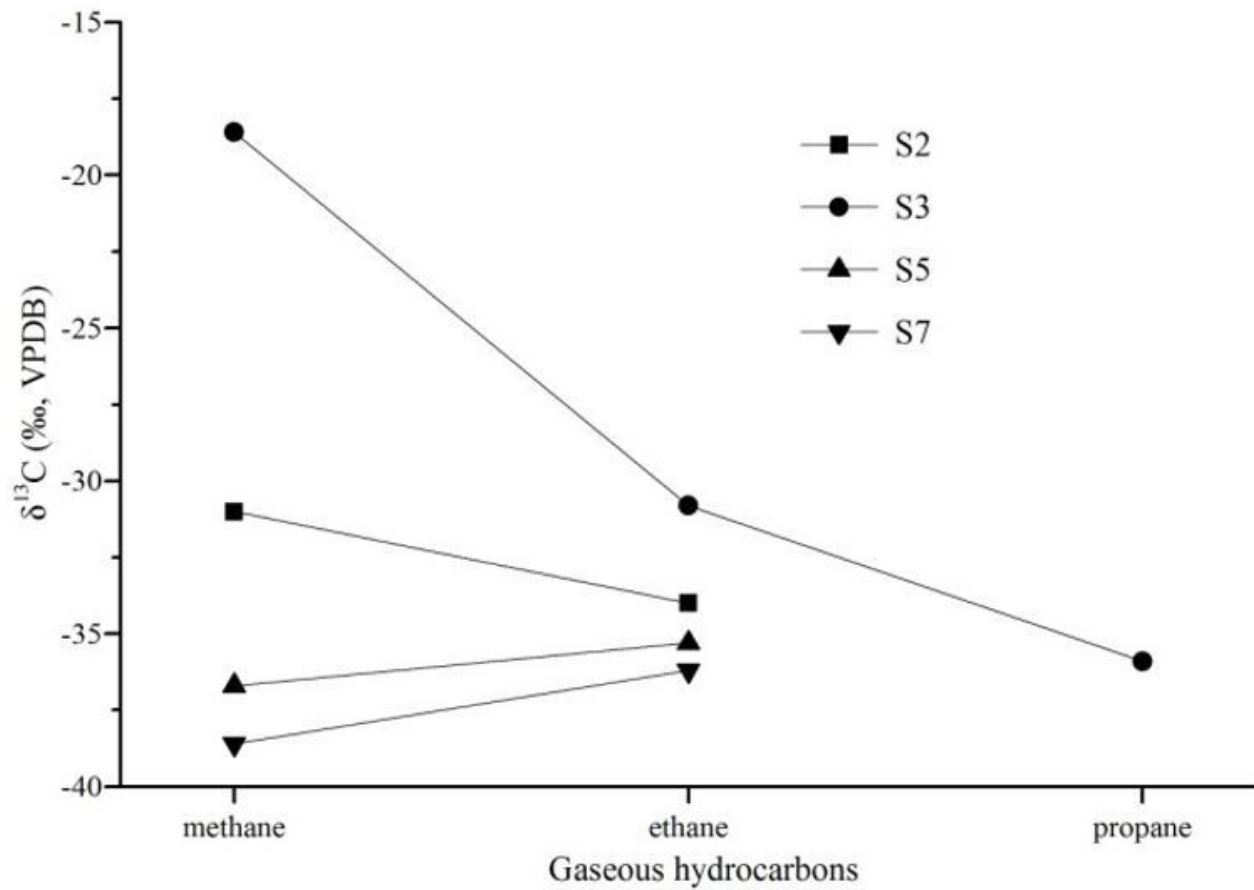


Figure 3

Isotope distribution on $\delta^{13}\text{C}$ versus gaseous hydrocarbons.

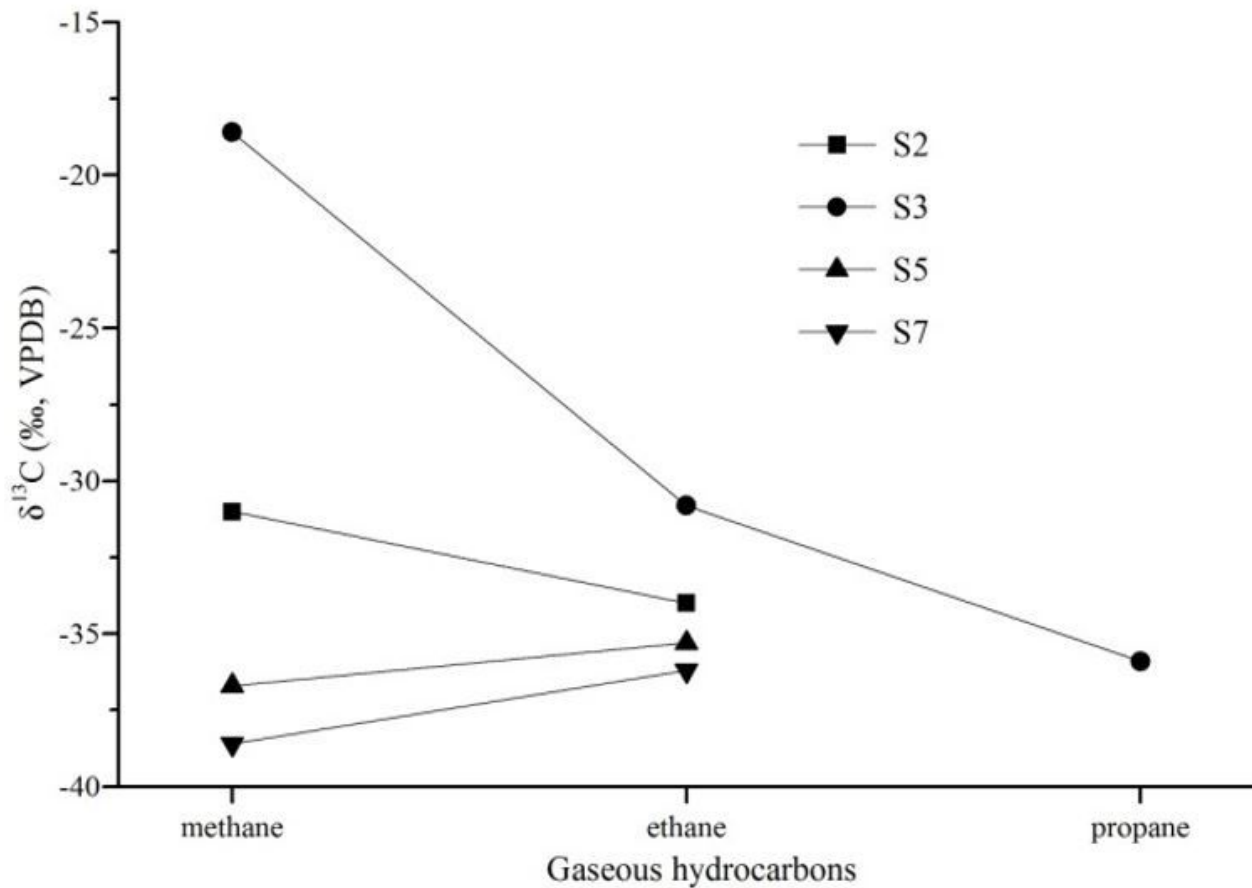


Figure 3

Isotope distribution on $\delta^{13}\text{C}$ versus gaseous hydrocarbons.

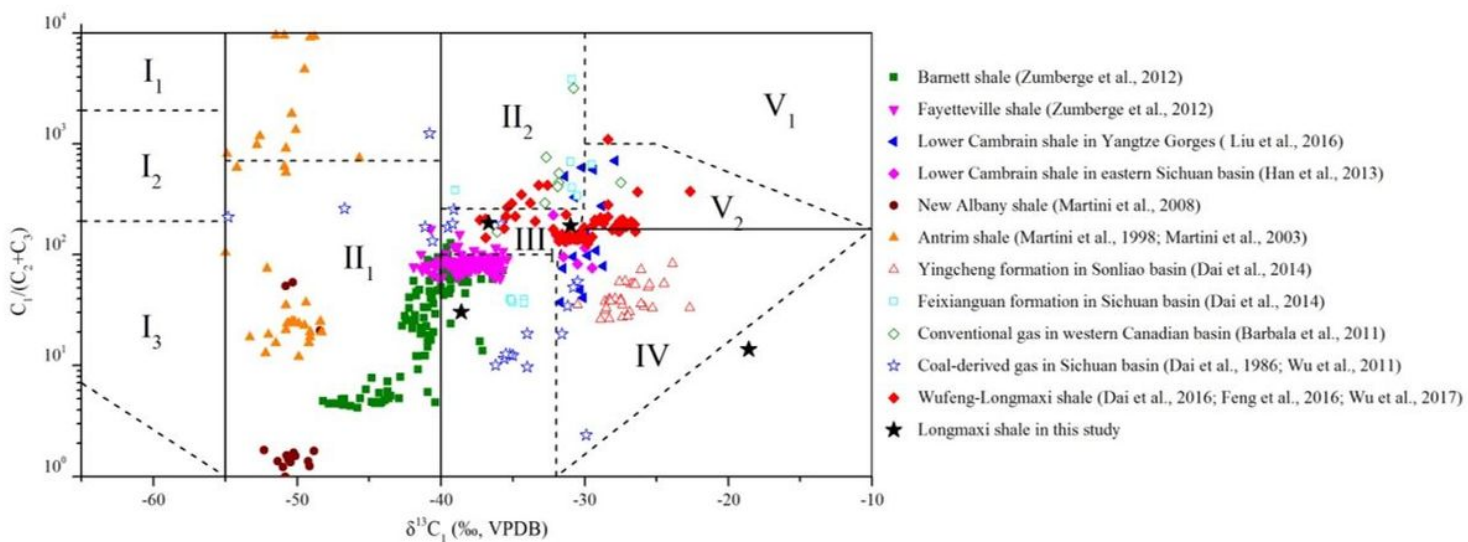


Figure 4

Cross plot of gas dryness ($C_1/(C_2+C_3)$) and $\delta^{13}\text{C}_1$.

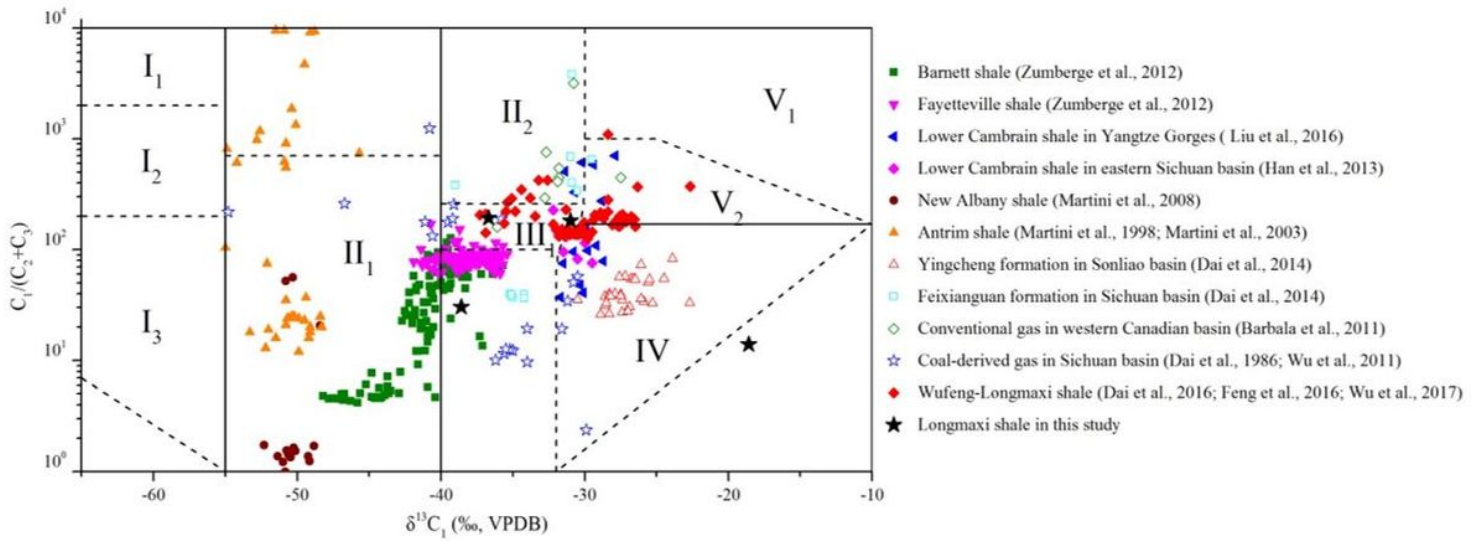


Figure 4

Cross plot of gas dryness ($C_1/(C_2+C_3)$) and $\delta^{13}C_1$.

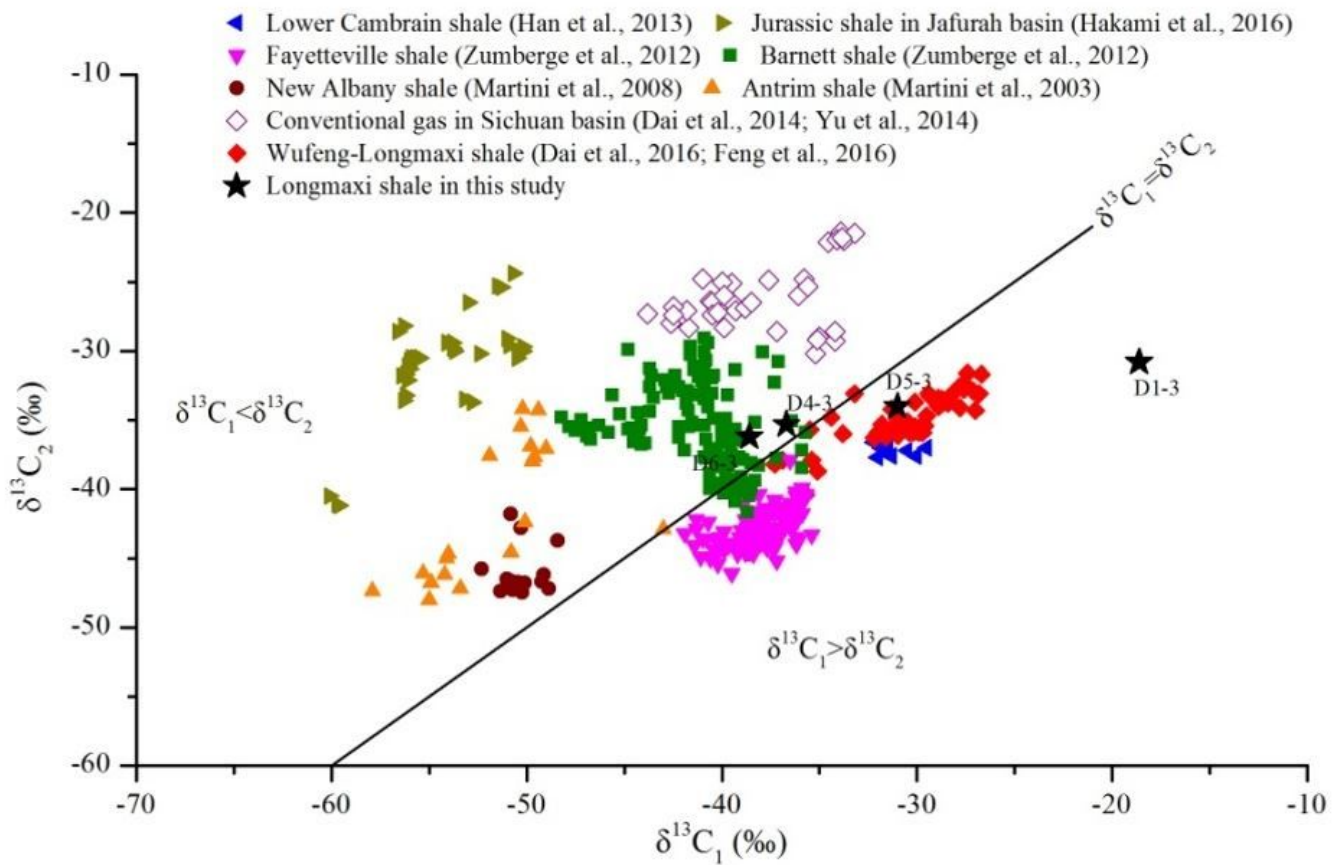


Figure 5

Cross plot of $\delta^{13}C_1$ and $\delta^{13}C_2$.

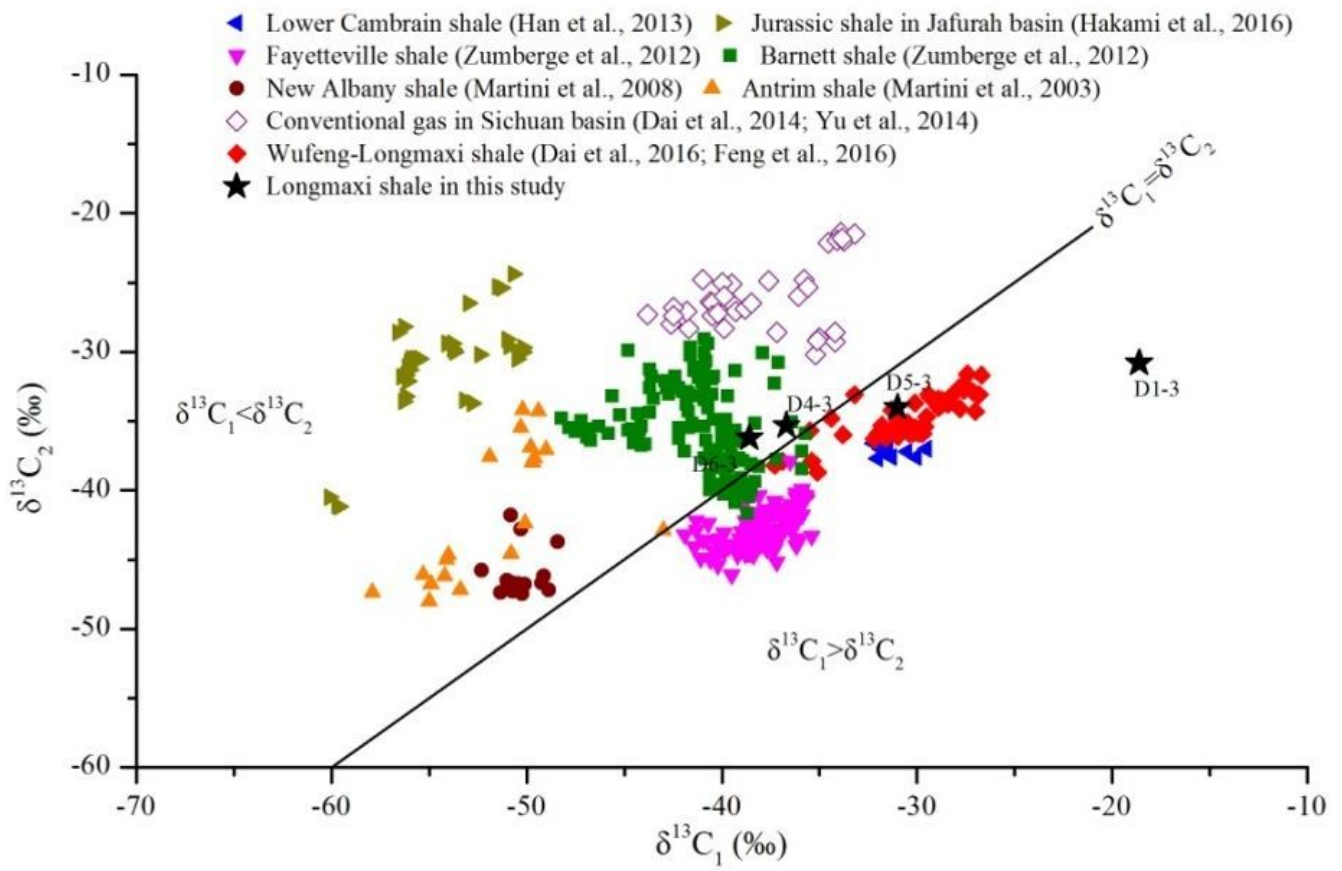


Figure 5

Cross plot of $\delta^{13}C_1$ and $\delta^{13}C_2$.

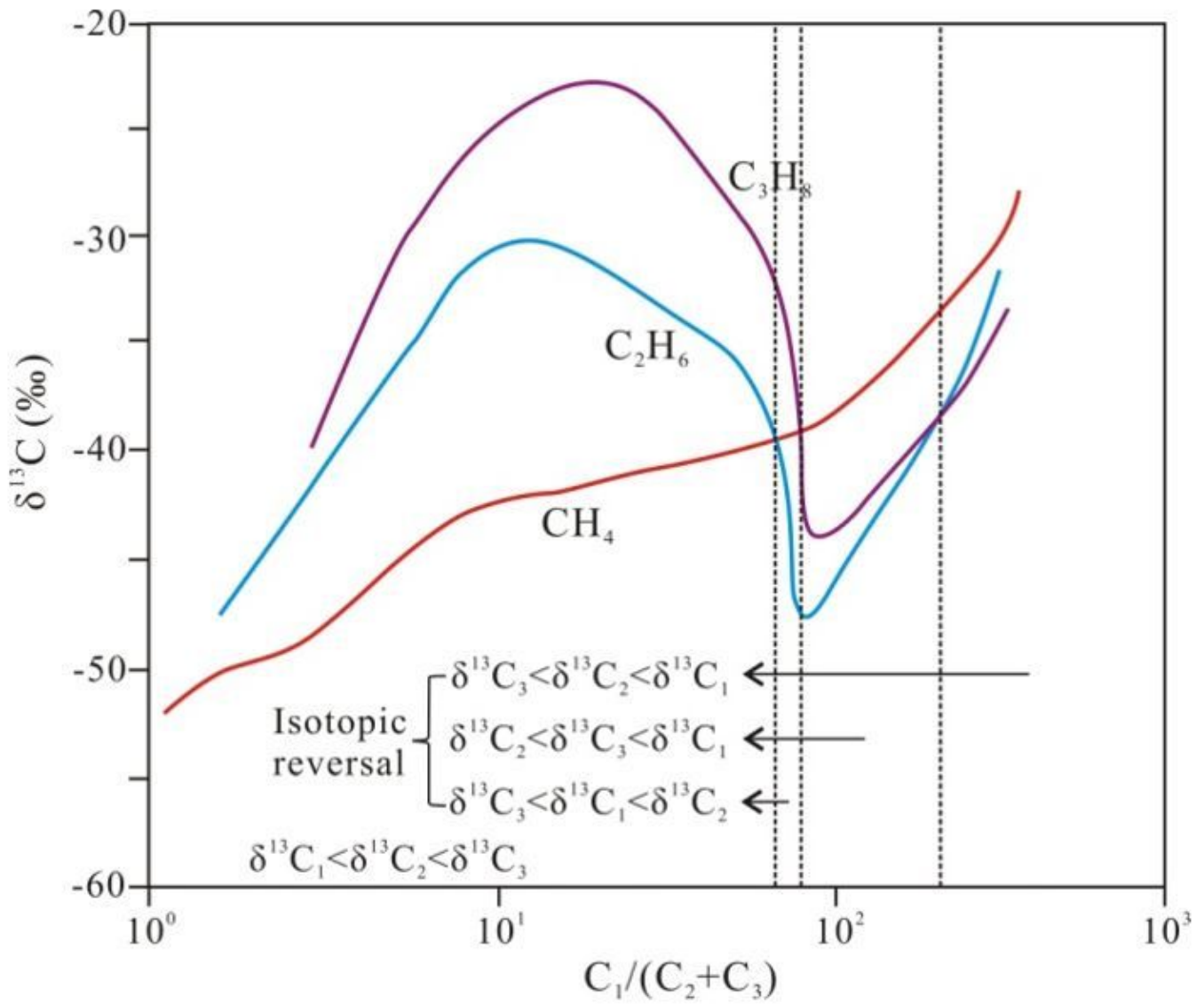


Figure 6

Relationship of $\delta^{13}\text{C}$ values of methane, ethane and propane and gas dryness ($C_1/(C_2+C_3)$) (revised from Zhao et al., 2016).

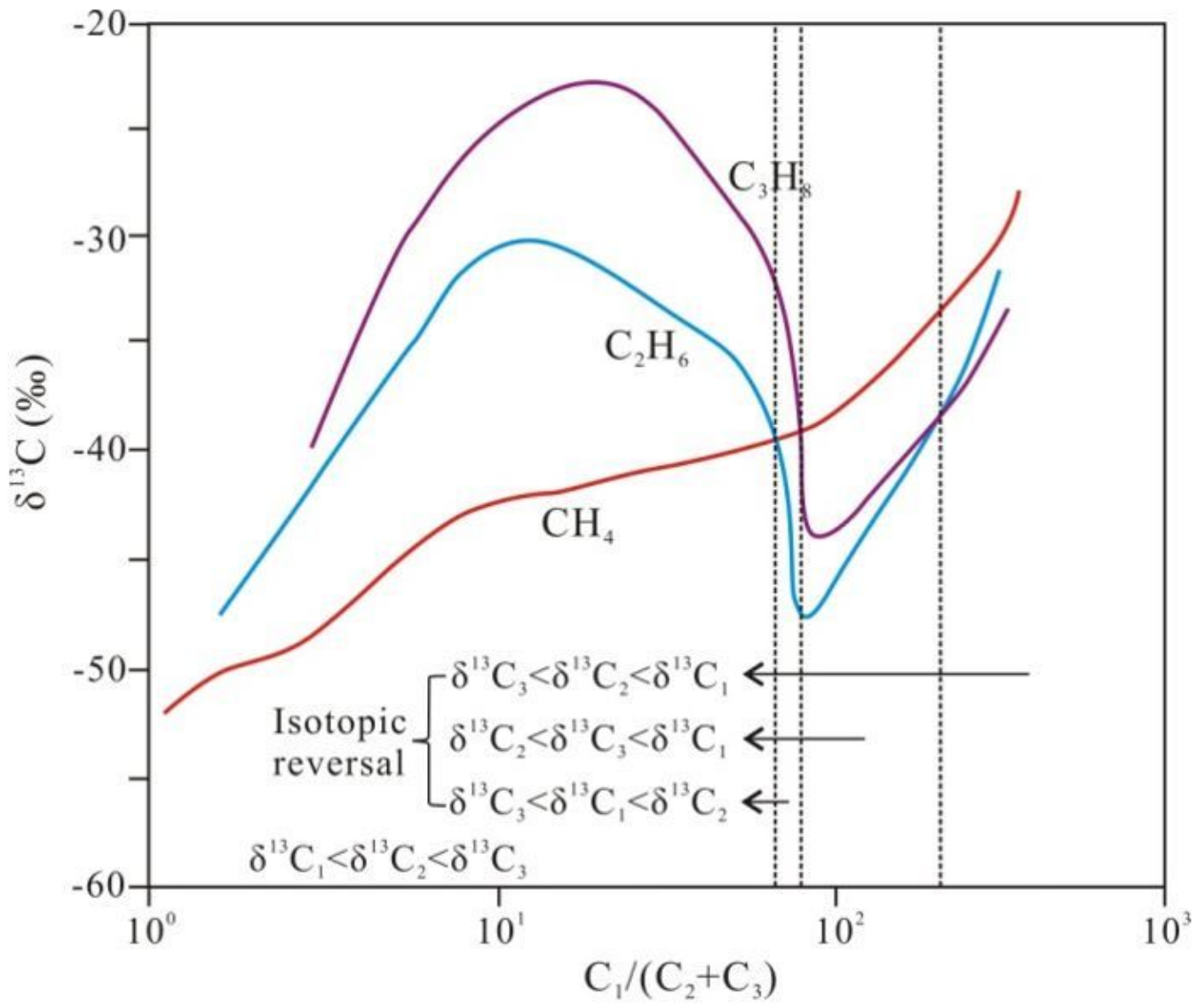


Figure 6

Relationship of $\delta^{13}\text{C}$ values of methane, ethane and propane and gas dryness ($C_1/(C_2+C_3)$) (revised from Zhao et al., 2016).

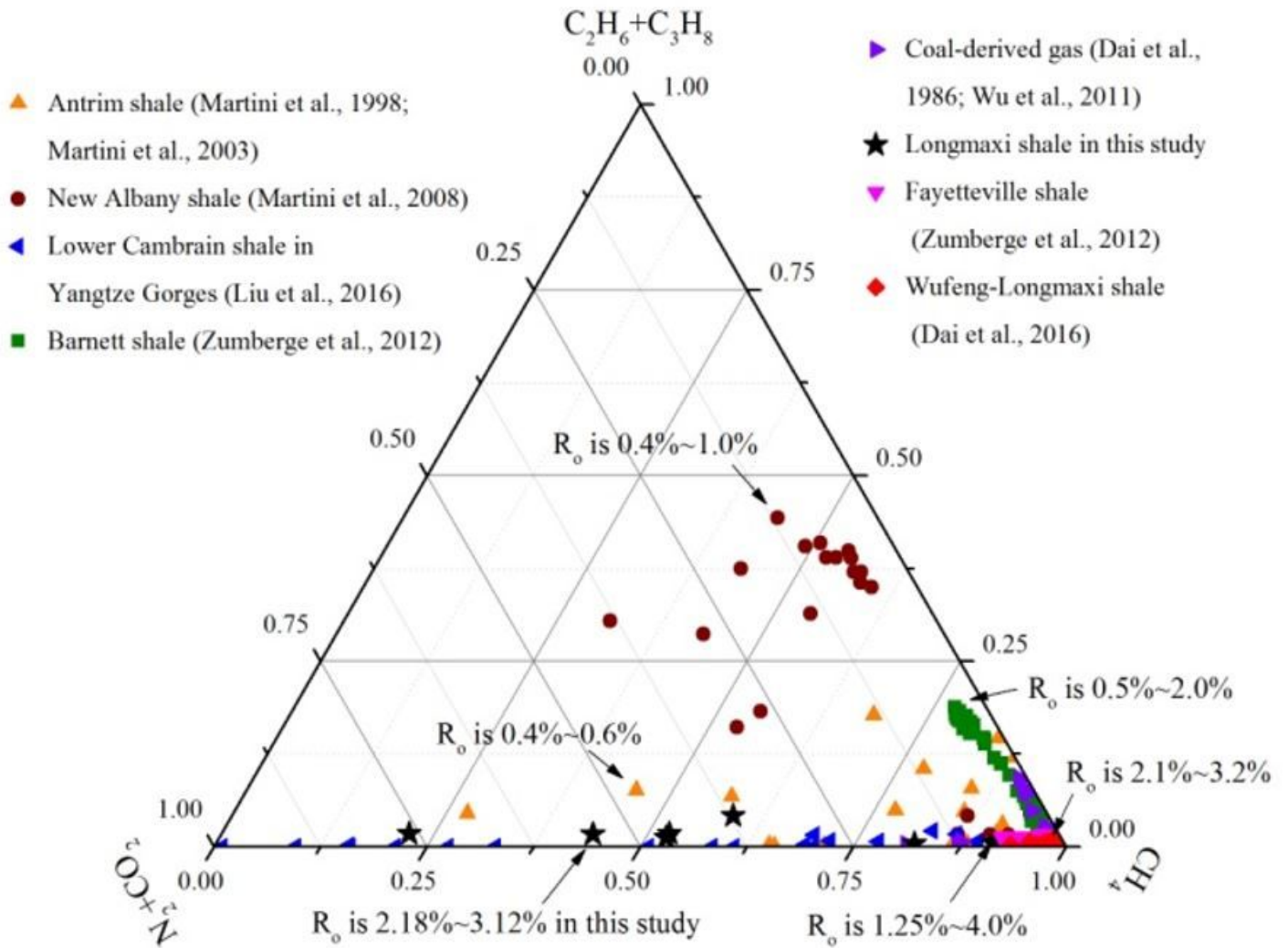


Figure 7

Ternary plot of shale gas components.

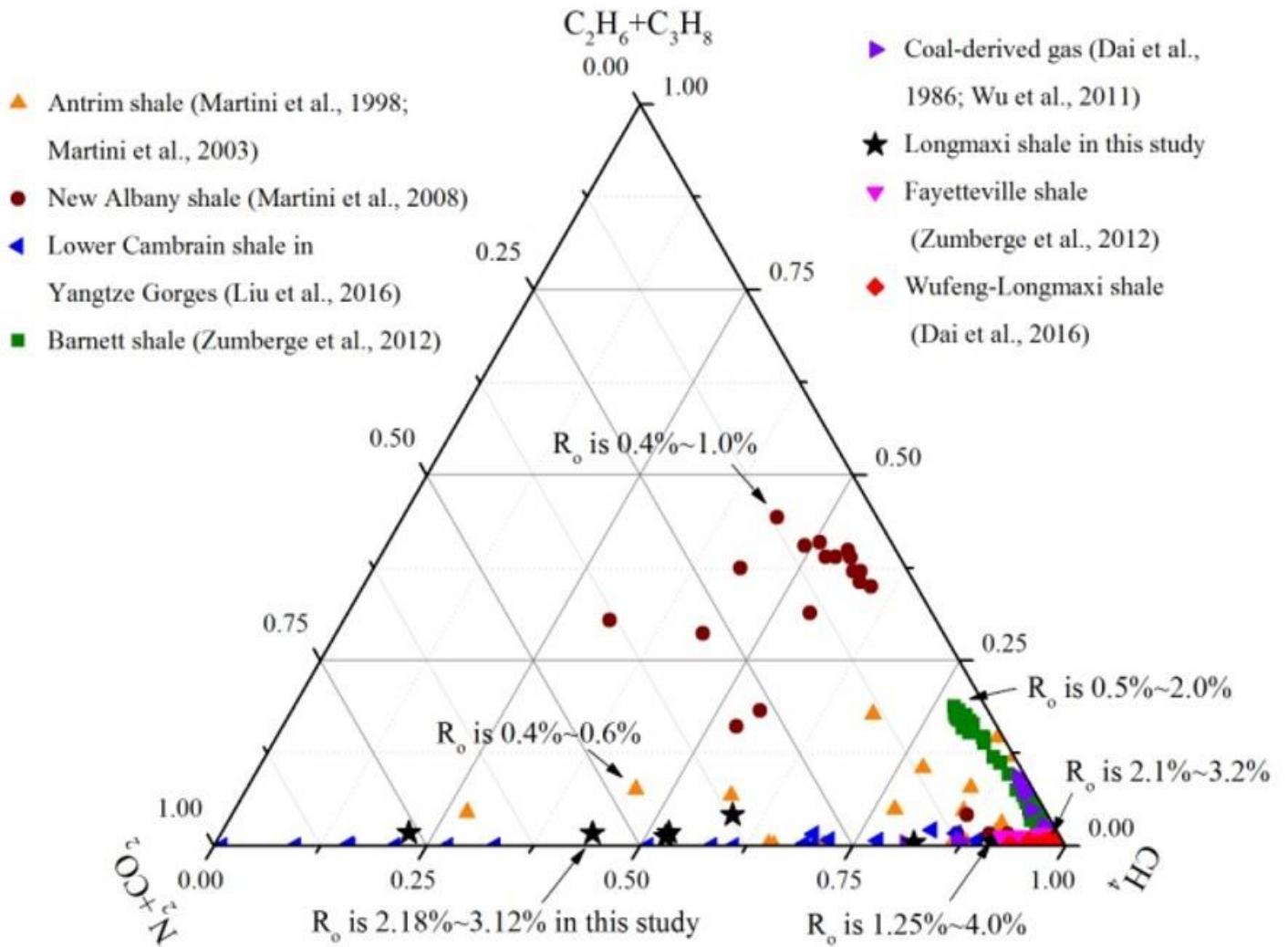


Figure 7

Ternary plot of shale gas components.